Rivista Italiana di Paleontologia e Stratigrafia
(*Research in Paleontology and Stratigraphy*)
vol. 123(1): 39-50. **March 2017**

STRONTIUM ISOTOPE STRATIGRAPHY AS A CONTRIBUTION FOR DATING MIOCENE SHELF CARBONATES (S. MARINO FM., NORTHERN APENNINES)

CLAUDIO ARGENTINO[1], MATTEO REGHIZZI[2], STEFANO CONTI[1], CHIARA FIORONI[1], DANIELA FONTANA[1*] & AURA CECILIA SALOCCHI[1]

[1*]Corresponding author. Dipartimento di Scienze Chimiche e Geologiche, Università di Modena e Reggio Emilia, Via Campi 103, 41125 Modena, Italy.
[2]Dipartimento di Fisica e Scienze della Terra, Università di Parma, Parco Area delle Scienze, 157/A, 43100 Parma, Italy.

To cite this article: Argentino C., Reghizzi M., Conti S., Fioroni C., Fontana D. & Salocchi A.C. (2017) - Strontium isotope stratigraphy as a contribution for dating Miocene shelf carbonates (S. Marino Fm., northern Apennines). *Riv. It. Paleontol. Strat.* 123(1): 39-50.

Key words: Strontium stratigraphy; shallow-water carbonates; Epiligurian; Miocene; northern Apennines.

Abstract. This paper provides new data on strontium isotope stratigraphy applied to the Miocene heterozoan shelfal carbonates of the S. Marino Fm. (Marecchia Valley, northern Apennines). Sr isotopic analyses were carried out on oyster shells, bryozoans and bulk-rocks from the lower-middle carbonate portion of the section. In the upper part of the succession that shows evidence of detrital influx, $^{87}Sr/^{86}Sr$ analyses were performed on foraminifera tests, separating planktonic and benthic forms. Results were compared with calcareous nannofossil biostratigraphic data from the same levels, in order to test the reliability of Sr dating in mixed carbonate-siliciclastic sediments. Mean ages obtained from oysters range between 16.9 Ma and 16.3 Ma. Very similar results are obtained using bryozoans (16.5 Ma to 16.1 Ma) and bulk-rocks (16.8 Ma to 16.2 Ma). These results allow to better constrain the age of the massive carbonate shelf, referable to the upper Burdigalian. In the upper carbonate-siliciclastic portion of the shelf, numerical ages obtained from planktonic and benthic foraminifera are in good agreement with nannofossil biozones (mean ages respectively around 15.3 Ma and 14.5 Ma) although they display wide confidence intervals. These wide age uncertainties depend on the slow rate of change of marine $^{87}Sr/^{86}Sr$ through time that characterizes the interval between ~15 and ~13.5 Ma.

Introduction

Miocene shallow-water carbonates are crucial for paleoclimatic and paleoenvironmental reconstructions in the Mediterranean area (Carannante & Simone 1996; Betzler et al. 1997; Bernoulli 2001; Bassant et al. 2005; Braga et al. 2006; Benisek et al. 2009; Pomar et al. 2012; Martinus et al. 2013; Brandano & Ronca 2014) but accurate correlations are limited by the generally poor age resolution in dating these deposits (Mutti et al. 2010; Reuter et al. 2013). Biostratigraphy is successfully applied in dating fine-grained basinal sediments, but is of limited applicability in shallow-marine carbonates because of the scarcity of useful markers. In these shelfal deposits a more precise dating can be reached by integrating different techniques.

During the last years the resolution of Sr isotope stratigraphy improved considerably, following the advancement in instrumentations and preparation techniques, making it a useful tool for correlation and dating of marine Phanerozoic carbonates (De Paolo & Ingram 1985; Howarth & McArthur 1997; Capo et al. 1998). This technique is based on the assumption that Sr signature of ocean water is homogeneous because residence time of Sr in seawater is far longer than ocean mixing time (McArthur 1994; Kroeger et al. 2007). Sr signature of global seawater is mainly controlled by the rate of weathering of continental silicate rocks rich in ^{87}Rb, that allows high ^{87}Sr inputs, and by the variable activity of mid-ocean volcanic ridges that provides light values (Krabbenhöft et al. 2010). Variations of the marine Sr composition through geological time have been tested and constrained with data obtained by biostratigraphy, magnetostratigraphy and astrochronology, and then interpolated with a LOWESS function in order to obtain a best-fit curve (Howarth & McArthur 1997; McArthur et al. 2001). Marine carbonates reflect the strontium isotopic composition of ambient seawater, if not affected by diagenesis, allowing to determine the time of mineral formation.

Received: July 22, 2016; accepted: December 15, 2016

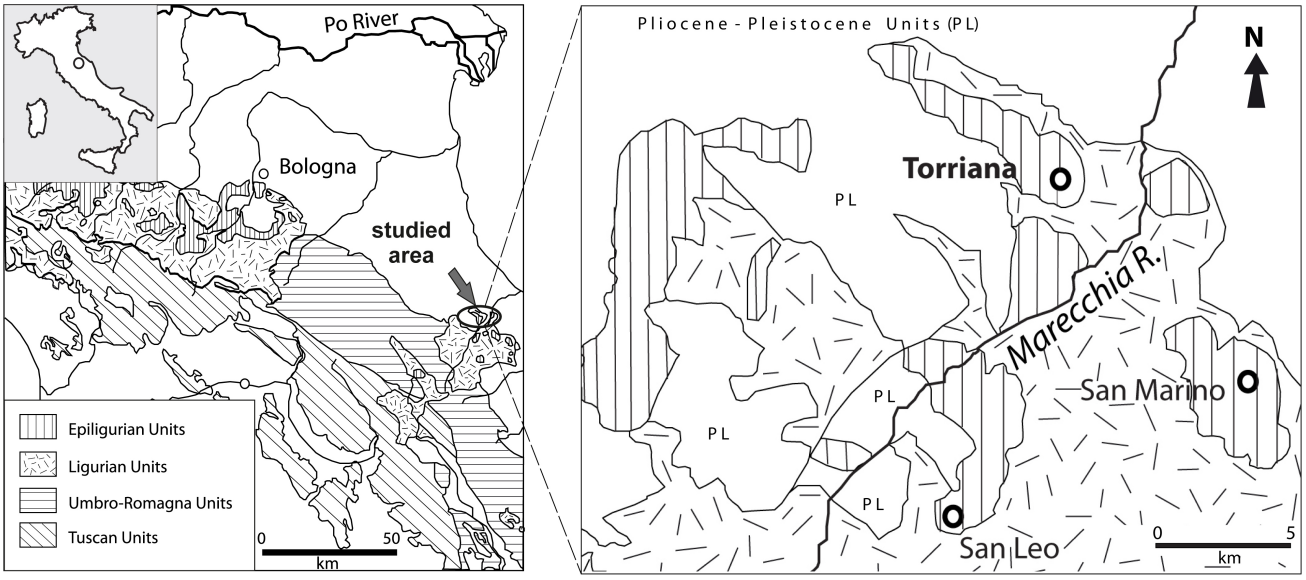

Fig. 1 - Schematic geological map of the Val Marecchia (northern Apennines) and location of the studied area (Torriana).

This method has been recently applied to Miocene Mediterranean carbonates providing significant age constraints (Scasso et al. 2001; Brandano & Policicchio 2012; Vescogni et al. 2014). The $^{87}Sr/^{86}Sr$ values are preferably measured on pectinid shells and oysters, which in several studies have testified their high preservation potential and reliability (Schneider et al. 2009). Both have a foliated structure composed of low-Mg calcite assumed to better retain the primary geochemical composition (Longman 1980; Veizer 1983; Marshall 1992; Freitas et al. 2006, 2008).

In this study we apply strontium isotope stratigraphy to the Miocene shelf carbonates of the S. Marino Fm. (Marecchia Valley, northern Apennines). Various works focused on the sedimentology and paleoenvironmental interpretation of this formation (Ricci Lucchi 1964; Amorosi 1997; Fontana et al. 2015; Conti et al. 2016), but there are still uncertainties on its precise age, in particular for the massive carbonate basal portion barren of planktonic markers.

Sr isotopic analyses were carried out on oyster shells, bryozoans and bulk-rocks sampled in carbonates from the well-exposed section of Torriana (Fig. 1). The upper part of the carbonate succession shows evidence of detrital influx and gradually passes to hybrid arenites and siltstones. This portion has been included in the isotopic study although bulk-rock measurements can be affected by detrital siliciclastic contamination. In this upper section Sr isotopes were performed on foraminiferal tests, separating planktonic and benthic forms. Results from these samples were compared with calcareous nannofossil biostratigraphic data from the same levels (Fontana et al. 2015), in order to test the reliability of Sr isotope dating in mixed carbonate-siliciclastic sediments.

Geological framework

The northern Apennines fold-thrust belt is located in the central part of the Mediterranean collisional system and developed since the Oligocene as a consequence of the collision between Adria and Corsica-Sardinia microplates (Marroni & Pandolfi 2007; Molli 2008). During the collision, the internal oceanic Ligurian units, representing the remnants of the Alpine Tethys, were thrusted over the western continental margin of Adria, overriding the Tuscan and Umbro-Marchean units (Ricci Lucchi 1990) (Fig. 1). During the migration of the accretionary wedge-foreland system, Ligurian units maintained the uppermost structural position of the orogenic wedge, with deposition occurring in small Epiligurian basins located on top of them (Ricci Lucchi 1986). The Epiligurian succession is subdivided by various unconformities in depositional sequences representing the infilling of wedge-top basins. Above the main Burdigalian unconformity, the Epiligurian sequence starts with transgressive

shallow-water carbonates from eastern Monferrato to Tuscan-Marchean Apennines (Amorosi 1997; Bicchi et al. 2006; Conti et al. 2008, 2016).

The S. Marino Fm. examined in this work occurs on top of the Val Marecchia thrust-sheet that mainly consists of stacked slices of Ligurian units overthrusting both Tuscan and Umbro-Marchean units (Conti et al. 2017 and references therein). The S. Marino Fm. crops out in numerous tabular and arcuate slabs that unconformably overlay the basal portion of the Ligurian units. In the Torriana arcuate slab (Fig. 1), the sedimentary infilling comprises a wedge-shaped Neogene succession capped by lower Pliocene deposits in the back portion of the arc. The total thickness is 150 m in the frontal portion, and up to 500 m in the rear part. Bedding planes are always S-SW-dipping with progressively lower inclination from the front to the back. Shelfal carbonates consist of shallow-water biogenic limestones, passing toward the top to hybrid arenites, arenites and siltstones that mark the drowning of the shelf.

The S. Marino Fm.: previous age determinations

The age of the S. Marino Fm. has been discussed by several authors but, due to the scarcity of biostratigraphic markers, the onset of the carbonate sedimentation is still uncertain, broadly attributed to the Burdigalian and/or Langhian (Ruggieri 1954; Ricci Lucchi 1964; Conti 1990; Amorosi 1997; De Capoa et al. 2015). The angular unconformity at the base of the S. Marino Fm. coincides with a major tectonic phase referred to the upper Burdigalian, but the temporal extent of the discontinuity is not defined in detail. Biostratigraphic nannofossil analyses carried out in the studied area did not yield data, because most of samples are barren. The comparison with other Miocene transgressive shelf carbonates outcropping from the back-arc to the foreland sectors of the Apennine chain indicates a wide age interval ranging from the Burdigalian to the Langhian (Amorosi 1997; Bicchi et al. 2006; Benisek et al. 2009; Reuter et al. 2013); therefore the precise age of the onset of the lower portion of carbonates remains uncertain.

Conversely, analyses on the upper portion of the succession, corresponding to hybrid and marly lithofacies, contain a well-diversified and rich nannofossil assemblage characterized by the presence of *Sphenolithus heteromorphus* and the absence of *Helicosphaera walbersdorfensis* (Fontana et al. 2015). These associations have allowed to assign this interval to the MNN5a (biostratigraphic zonation of Fornaciari et al. 1996) corresponding to the lower Langhian, thus constraining the age of the top of the S. Marino Fm.

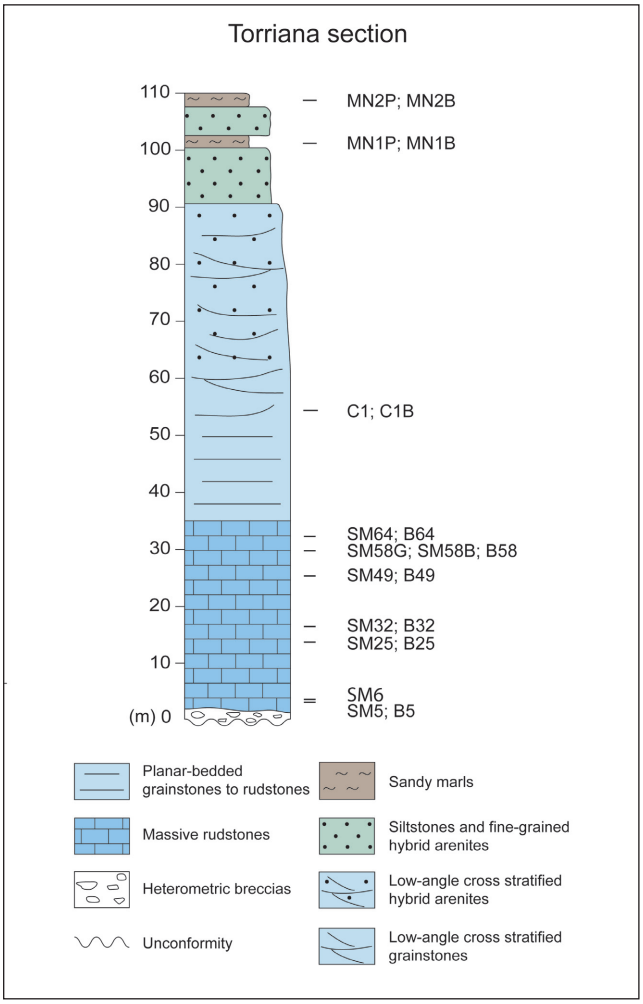

Fig. 2 - Lithostratigraphy of the Torriana section (modified from Salocchi et al. 2017) with location of samples for Sr isotope analyses.

The Torriana section

The sampling for the isotopic study has been carried out in the Torriana section, located in a dismissed quarry area in proximity of the homonymous town (43°59'15"N, 12°22'59"E), where the S. Marino Fm. is well exposed from the basal unconformity to the upper fine-grained lithologies. The succession, studied in detail by Salocchi

Fig. 3 - A) The lower-middle portion of the Torriana section. B) Polygenic breccias at the base of the succession. C) Close-up of the massive carbonate facies; white patches are bryozoan colonies. D) Cross-bedded hybrid arenites. E) Passage from the hybrid arenites to siltstones and sandy marls in the upper portion of the succession.

et al. (2017), consists of different lithofacies for a thickness of 110 m (Figs 2, 3A).

The section starts with a polygenic breccia, 2 m thick, made up of well-cemented coarse-grained pebbles of various composition (limestones and siltstones) deriving from the underlying allochtonous Ligurian units (Fig. 3B). Rudstones and grainstones constitute a massive interval 35 m thick; the main biogenic components are represented by bryozoans and echinoids (Figs 3C, 4A); local concentrations of bivalves, oysters and pectinids, are observed. Red algae and larger benthic foraminifera are subordinated. Planar-bedded grainstones to packstones characterize the interval between 35 m and 54 m. They gradually pass to low angle cross-stratified grainstones up to 90 m (Fig. 3D). The interval 64-90 m is characterized by abundant fine-grained sandy fraction, usually concentrated in thin laminae, and represents the transition to fine-grained hybrid-arenites, siltstones and sandy marls rich in glauconites and planktonic foraminifera (90-110 m) (Figs 3E, 4B).

Materials and methods

Sr isotope analyses were performed using different material and methodologies for the carbonate basal-middle portion of the section (a) and the upper carbonate-siliciclastic part (b).

a) In the carbonate portion, Sr isotope analyses were performed on bioclasts and bulk-rocks. 16 samples were selected: 4 oyster shells, 4 bryozoans, 1 crinoid and 7 bulk-rocks, sampled at different stratigraphic levels, from 3.5 m to 55 m (Fig. 2). Fossil specimens were selected on thin-section counterpart and then sampled using a micro-drill, avoiding altered portions. Oyster shells were previously examined in thin section and by scanning electron microscope in order to assess the textural preservation and to detect possible secondary precipitates indicative of recrystallization.

About 20 mg of powder were collected for geochemical analysis using a micro-drill. Powdered samples were rinsed three times with MilliQ water. After drying, each sample was leached two times using a solution of 0.3% w/w acetic acid, in order to sequentially dissolve about 30% and 40% of powdered material, following the procedure described in Li et al. (2011) and successfully applied by Palmiotto et al. (2013) and Vescogni et al. (2014). Solutions were dried down and reacidified in 3 ml of 3 M HNO_3.

b) In the upper carbonate-siliciclastic portion two samples were collected from the sandy marls at 102 m and 108 m (Fig. 2). Due to the lack of macrofossils, we analyzed foraminifera separating planktonic and benthic forms (mainly hyaline), without taxonomic

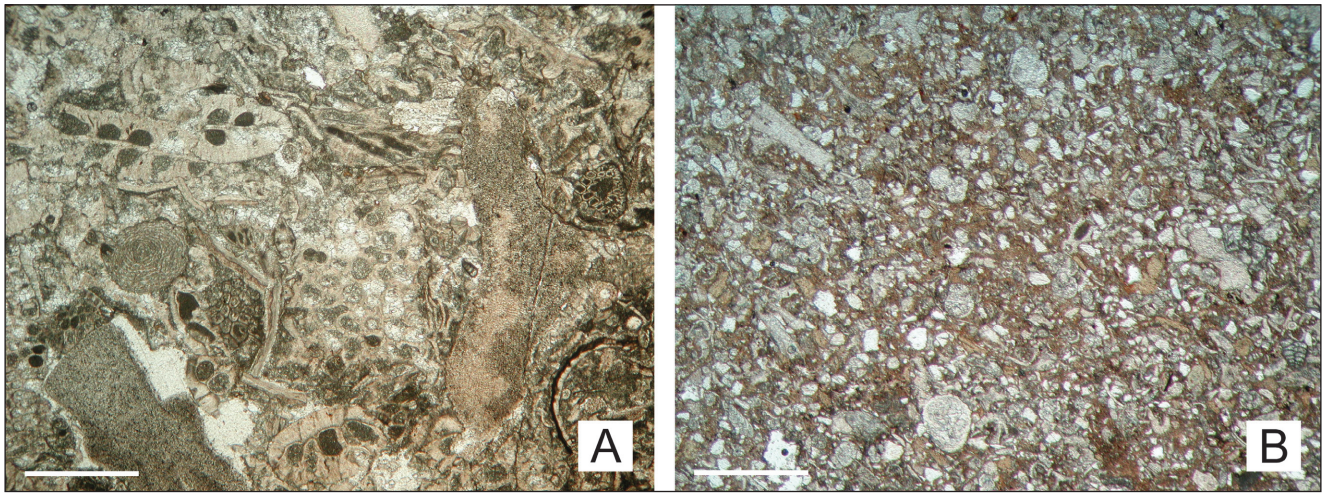

Fig. 4 - A) Photomicrograph of the massive lithofacies composed of bryozoans, echinoid plates and large benthic foraminifera (sample SM25 at 13.5 m). B) Fine-grained arenites in the upper portion of the succession with an abundant siliciclastic fraction and planktonic foraminifera (sample MN1, at 102 m). Scale bar = 1 mm.

distinction. Rock samples were dried in oven at 60°C for approximately 48h and disaggregated by soaking in distilled water. Material was washed through sieves to remove the mud fraction. The residue was dried and newly sieved to separate the sand-sized grains. Planktonic and benthic foraminifera tests were picked providing 4 subsamples. Each subsample consists of at least 100 specimens (~1.0 mg) of foraminifera, hand-picked from the >125 μm fraction. Specimens were ultrasonically washed in MilliQ water for 10 minutes to remove residual particles and leached with 0.01 M HCl to etch the outer surface and to dissolve possible carbonate contaminants. Samples were then dissolved in 0.5 ml of 5 M-acetic acid to minimize the dissolution of siliciclastic contaminants. Solutions were centrifuged to check the presence and remove any insoluble residue, dried down and reacidified in 3 ml of 3 M HNO_3.

Strontium ions from all the samples were isolated from the carbonate matrix using Eichrom Sr-SPEC resin, following the method reported in Palmiotto et al. (2013). Final solutions were adjusted to a concentration of 4% w/w HNO_3 and analyzed within a few days. Strontium isotope ratios were obtained using a high resolution multi collector inductively coupled plasma mass spectrometer (HR-MC-ICPMS Thermo Scientific™ Neptune), housed at CIGS Unimore. Strontium content was previously tested by using a quadrupole inductively coupled plasma mass spectrometer, (ICPMS X Series II, Thermo Fisher Scientific).

Bioclast (oyster shells, bryozoans and crinoid) samples were diluted to 125 ppb and introduced into the Neptune with the standard inlet system (cyclonic spray chamber and a 100 μl/min nebulizer). The sensitivity for 125 ppb Sr was 6 V on the ^{88}Sr peak and the blank level (4% w/w HNO3) was < 0.01 V. Because of the scarce amount of material (and consequently low Sr signal), foraminifera sample solutions were introduced into the Neptune via a high sensitivity desolvating inlet system ESI-APEX IR and a 100 μl/min nebulizer. The sensitivity for 30 ppb Sr was 5 V on the ^{88}Sr peak and the blank level (4% w/w HNO3) was < 0.04 V.

Analytical $^{87}Sr/^{86}Sr$ determinations were corrected to a value of 0.710248 for strontium isotope standard NIST SRM 987 (McArthur et al. 2012). Samples, standards and blank solutions were analyzed in a static multi-collection mode in a single block of 100 cycles with an integration time of 8.389 s per cycle. Samples were analyzed using a bracketing sequence (blank/standard/blank/sample/blank) to correct possible instrumental drifts. The $^{87}Sr/^{86}Sr$ ratios were corrected for mass fractionation (mass bias) effect using $^{88}Sr/^{86}Sr = 8.37520$ as normalizing ratio and an exponential law (Steiger & Jäger 1997). Isobaric interferences of ^{86}Kr and ^{87}Rb on ^{86}Sr and ^{87}Sr species respectively were considered. Finally, values obtained for NIST SRM 987 Sr standard measured before and after each samples in the bracketing sequence were used for C-factor calculation ("C-factor" = true isotope ratio (i.e. 0.710248) divided by the average value of the two standards measured). Each sample isotope ratio has been multiplied by the obtained C-factor value to be corrected for possible instrumental drift. For the March 2015 analytical session, repeated measurements of NIST SRM 987 gave a mean value of 0.710256 ± 0.000038 (2 S.D., n = 16), whereas for the April 2016 session it was 0.710237 ± 0.000054 (2 S.D., n = 9).

$^{87}Sr/^{86}Sr$ values were converted into numerical ages using the regression curve LOWESS look-up Table version 5 (McArthur pers. com.).

Results

Material preservation

Diagenetic screening has been performed prior to Sr analysis in order to verify that the carbonate material was pristine and retained the primary isotopic signal. SEM analyses of the oyster shells show a well-preserved foliated microstructure and smooth layers surfaces, without evidence of recrystallization (Fig. 5A, B). Structures are comparable to that of modern oysters (Ullmann et al. 2013; Ullmann & Korte 2015) and therefore indicative of good preservation. Bryozoan fragments in transversal section range from few millimetres to centimetres and show thick outer walls consisting of brownish fibrous calcite (Fig. 4A). Zooecial diameter is < 300 μm and mainly filled by micrite. The crinoid ossicle is cloudy in appearance with a small round *lumen*.

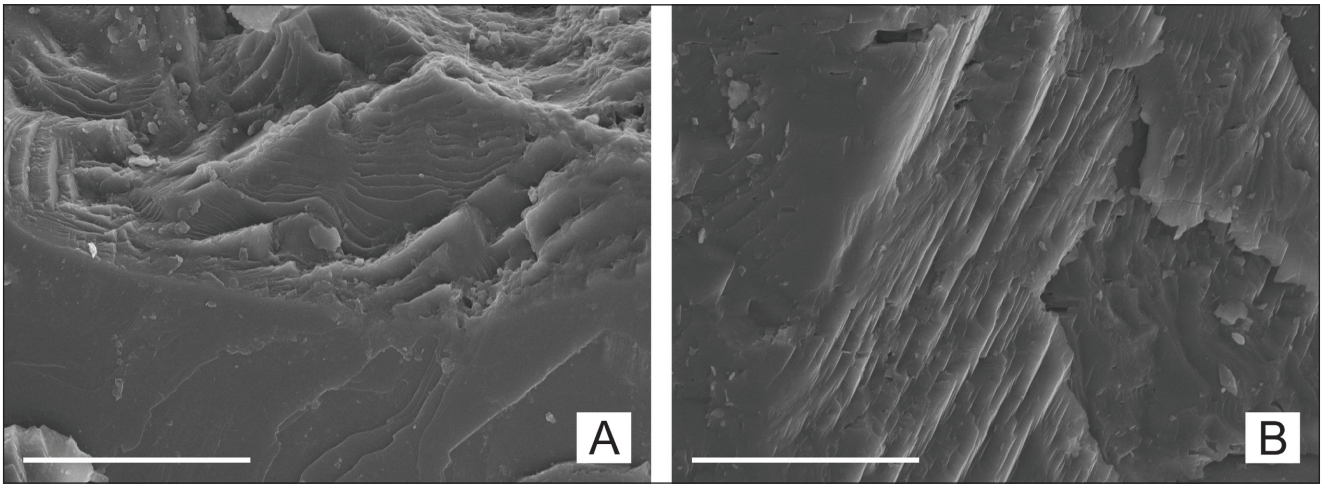

Fig. 5 - SEM microphotographs of oyster shell fragments from the massive carbonate lithofacies showing a well preserved foliated microstructure and smooth surfaces. Sample SM5 (A) and sample SM58G (B). Scale bar = 20 μm.

No abrasion features indicative of reworking have been observed.

Strontium isotope analytical results

Oyster shells, bryozoans and bulk-rocks from the carbonates in the basal-medium portion of the succession (3.5-33 m) yielded mean $^{87}Sr/^{86}Sr$ ratios between 0.708664 and 0.708721, that converted to numerical ages correspond respectively to 16.9 ± 0.6 Ma and 16.1 ± 0.6 Ma (Fig. 6, Tab. 1). The different carbonate components show very similar values. Ages obtained from oyster shells span from 16.9 ± 0.6 Ma to 16.3 ± 0.6 Ma. Bryozoans yield comparable values ranging from 16.5 ± 0.6 Ma to 16.1 ± 0.6 Ma. In particular samples SM6 and SM58B show the same mean age. Bulk-rock values range from 16.8 ± 0.6 Ma to 16.2 ± 0.6 Ma. Bulk-rock and bryozoans from the sample collected at 30 m (B58 and SM58B) provided the same value. One crinoid sample (C1, sampled at 55 m, Fig. 2) corresponds to an age of 16.1 ± 0.9 Ma. The bulk-rock indicates 12.3 ± 2.8 Ma.

Benthic foraminifera from samples MN1 and MN2 (Tab.1) gave similar mean values, respectively 14.6 Ma and 14.5 Ma. Planktonic tests from the same samples show different values if considering the mean ages (15.1 Ma and 15.6 Ma, respectively). Foraminifera yield large age uncertainties between ± 1.5 My and ± 2.4 My (Fig. 6).

Discussion

Our results allow to better constrain the age of the carbonate shelf (16.9 ± 0.6 Ma to 16.1 ± 0.6 Ma) referable to the Late Burdigalian. Isotopic

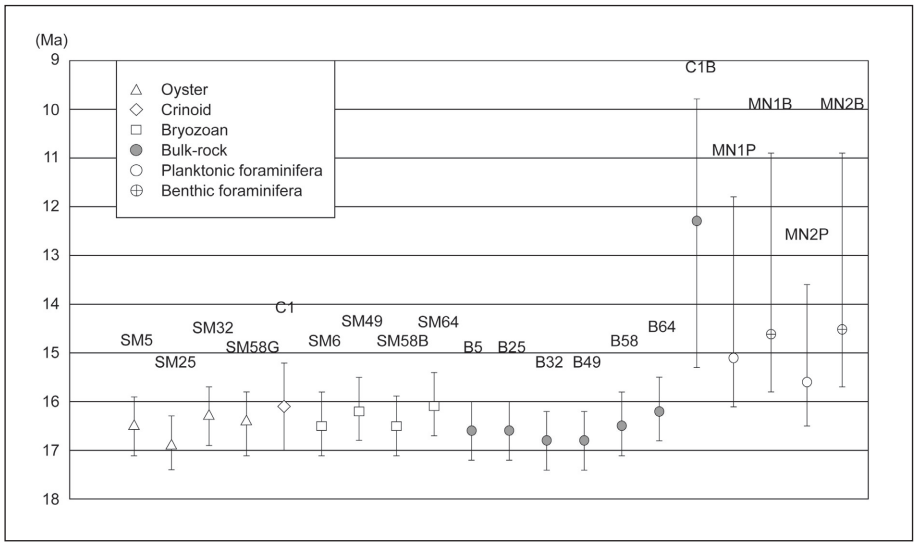

Fig. 6 - Strontium isotope ages of the Torriana samples and associated confidential limits for the analyzed components.

Tab. 1 - $^{87}Sr/^{86}Sr$ values and numerical ages for different carbonate materials. Maximum and minimum ages are obtained respectively subtracting and summing the cumulative error (reported in parenthesis) to mean isotopic value, and converted using the Look-up Table 5 (by McArthur pers. com.). The double standard error (2 S.E.) represents the internal analytical error of each measurement.

Sample	Material	$^{87}Sr/^{86}Sr$	2S.E.(*10^6)	Maximum age (Ma)	Mean age (Ma)	Minimum age (Ma)
SM 5	Oyster	0.708690 (39)	10	17.1	16.5	15.9
B 5	Bulk-rock	0.708685 (40)	11	17.2	16.6	16.0
SM 6	Bryozoan	0.708693 (41)	16	17.1	16.5	15.8
SM 25	Oyster	0.708664 (39)	8	17.4	16.9	16.3
B 25	Bulk-rock	0.708683 (39)	10	17.2	16.6	16.0
SM 32	Oyster	0.708703 (39)	9	16.9	16.3	15.7
B 32	Bulk-rock	0.708669 (39)	9	17.4	16.8	16.2
SM 49	Bryozoan	0.708714 (40)	12	16.8	16.2	15.5
B 49	Bulk-rock	0.708671 (39)	10	17.4	16.8	16.2
SM 58G	Oyster	0.708696 (41)	16	17.1	16.4	15.8
SM58B	Bryozoan	0.708693 (39)	8	17.1	16.5	15.9
B 58	Bulk-rock	0.708693 (39)	10	17.1	16.5	15.8
SM 64	Bryozoan	0.708721 (39)	11	16.7	16.1	15.4
B 64	Bulk-rock	0.708715 (39)	10	16.8	16.2	15.5
C 1	Crinoid	0.708718 (56)	15	17.0	16.1	15.2
C 1B	Bulk-rock	0.708833 (55)	14	15.3	12.3	9.8
MN 1P	Planktonic foram.	0.708781 (55)	12	16.1	15.1	11.8
MN 1B	Benthic foram.	0.708801 (55)	13	15.8	14.6	10.9
MN 2P	Planktonic foram.	0.708752 (55)	13	16.5	15.6	13.6
MN 2B	Benthic foram.	0.708803 (55)	12	15.7	14.5	10.9

values seem to follow a sort of stratigraphic distribution: the lowest samples give the oldest age (16.9 Ma) and the upper samples show youngest age (16.1 Ma) (Fig. 7). However, the confidential interval of each value partially overlaps and does not permit more precise considerations. The preservation of the primary geochemical signature is confirmed by the good consistency of the strontium isotope values of different carbonate components from the same stratigraphic level (Fig. 6).

The consistency between ages obtained from the oysters and those from bryozoans and the bulk-rock suggests that these last carbonate components could be potentially used for Sr isotopic studies when the diagenetic imprint of the rock is negligible. Only in the case of crinoid sample , we observed a difference between the ossicle (sample C1, 16.1 Ma) and the relative bulk-rock (sample C1B, 12.3 Ma). The latter may reflect the mixing of primary isotopic signal with the high $^{87}Sr/^{86}Sr$ ratio supplied by later pore-filling cement represented by sparry calcite, more abundant up in the section in correspondence of the first pulses of detrital material.

The upper portion of the succession is almost barren of oysters, and has a detrital siliciclastic fraction that could lead high Rb contaminations. Numerical ages obtained from Sr isotope analyses on foraminifera tests have wide confidence limits (2.9-4.9 My). Ages obtained from benthic foraminifera are around 14.5 Ma while planktonic foraminifera give values around 15.3 Ma; both are in good agreement with data reported in Fontana et al. (2015) based on nannofossil assemblages, that indicate the MNN5a subzone, Langhian in age (Fig. 7). The recrystallization of foraminifera tests can not be completely ruled out, as well as detrital contaminations, and this could partially explain the $^{87}Sr/^{86}Sr$ value discrepancies between benthic and planktonic samples belonging to the same stratigraphic level. A recrystallization effect of the original carbonate tests would likely be reflected by a more radiogenic signal, due to the increasing $^{87}Sr/^{86}Sr$ trend for the time interval considered. Also a detrital influence (that in the examined samples is mainly made up of quartz, feldspars, micas and clay matrix) could determine an increasing $^{87}Sr/^{86}Sr$ signal, due to the presence of clay minerals that incorporate Rb in concentrations of tens to hundreds of ppm (McArthur 2012).

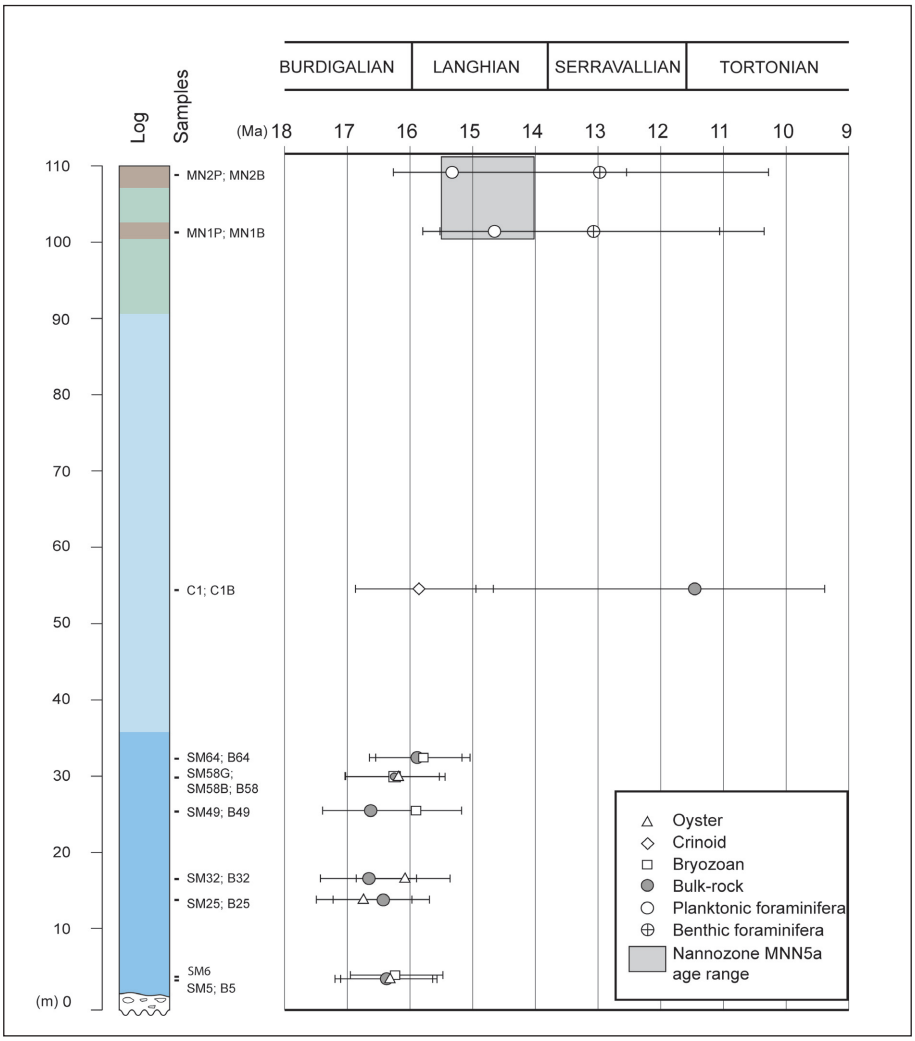

Fig. 7 - Strontium isotope ages plotted with their relative age confidence limits versus stratigraphy of the Torriana section (log colors refer to Fig. 2). In the upper part of the section Sr ages are compared with nannofossil data (biozone MNN5a, grey area; from Fontana et al. 2015).

The Sr isotope data in the upper part of the studied section are certainly influenced by the low slope of the calibration curve characterizing this time interval. A slow rate of change of marine $^{87}Sr/^{86}Sr$ through time determines a low slope of the regression curve and this does not allow a precise location of the measured ratios (on a flat line, the worst theoretical case, a single $^{87}Sr/^{86}Sr$ value would correspond to infinite numerical ages, McArthur 1994). The regression curve, which is representative of the $^{87}Sr/^{86}Sr$ values of seawater during the Miocene, has been described by a high order function with two distinct phases of increased slope related to the uplift and denudation of the Himalayan-Tibetan Plateau (Hodell & Woodruff 1994; McArthur et al. 2001). The early Miocene is characterized by a steep curve with $^{87}Sr/^{86}Sr$ growth rate of about 60 ppm/My until 19 Ma and 80 ppm/My during the interval 19-16 Ma. Then, the ratio shows a slight decrease during the time interval between ~15 Ma and ~13.5 Ma. Hence, the best age estimation attainable with the Sr method is expected for the Aquitanian to the lower Langhian time interval when the slope of the curve is steeper (Hodell & Woodruff 1994).

A further point to consider is the confidence limit associated to each value, which depends both on the slope of the fitting curve and on the density of calibration data points used for the line construction (McArthur 1994). Browning et al. (2013) estimated the theoretical maximum age resolution achievable in Miocene based on LOWESS fit of McArthur et al. (2001) and considering an external precision of 0.000008; they obtained good resolutions (about ± 0.25-0.5 My) from the interval 25 Ma to 15 Ma, significantly decreasing in sediments younger than 15 Ma (about ± 0.75-1.5 My). A direct correlation between mean ages and the width of the confidence interval can be observed in our data (Fig. 6). In fact, oyster samples from the lower part of the carbonate succession provided relatively narrow confidence intervals (around ± 0.6 My) compared to those obtained from younger foraminifera samples.

Our data indicate that the application of Sr isotopes represents a reliable and useful dating method that can be applied to carbonate platforms, mostly when a biostratigraphic approach is not applicable due to the lack of useful biomarkers. However, as widely discussed by Veizer et al. 1997 and recently by Eidvin et al. (2014), intrinsic limitations of this method have not to be undervalued. Precise age determinations can be achieved when the pristinity of the carbonate material is assessed through geochemical or optical techniques, in time intervals where the calibration curve has sufficient slope.

Conclusions

Sr isotope stratigraphy integrated with previous calcareous nannofossil biostratigraphy data has been applied to better constrain the age of the Miocene shelf carbonates of S. Marino Fm. (northern Apennines). Isotopic analyses were performed on different carbonate components (oysters, bryozoans and bulk-rocks) from the same stratigraphic levels. The reliability of the analytical results and the relatively low confidence limits permit to ascribe the lower and middle portion of the carbonate succession to 16.9 Ma and 16.1 Ma, corresponding to the upper Burdigalian.

The different bioclasts investigated from the same stratigraphic level provided similar $^{87}Sr/^{86}Sr$ values, supporting the consistency of the obtained ages.

Sr isotopic values from foraminifera (benthic and planktonic) from the upper portion of the succession, carbonate-siliciclastic in composition, provide numerical ages in agreement with the calcareous nannofossil biostratigraphy. However, Sr isotope ages from foraminifera show wide confidential intervals largely due to the low coefficient of the regression curve used for age conversion. Successful application of the Sr isotopes to the Miocene is limited to specific intervals corresponding to steep $^{87}Sr/^{86}Sr$ curve. Combination of Sr isotope stratigraphy on shelfal carbonate facies with biostratigraphy on marly intervals is a potential tool for dating carbonate platforms, allowing more precise stratigraphic correlations.

A more robust age definition of the S. Marino Fm. is important not only to improve knowledge of regional geology, but also for accurate correlations with other Miocene platforms in the Mediterranean and their significance in terms of paleoenvironmental and paleoclimatic events.

Acknowledgements. The work has been funded by MIUR (Italian Ministry of Research, project PRIN 2011 Grant 20107ESMX9: Demise and recovery of carbonate systems and their potential for reservoir generation: role of climate, tectonics and magmatism). We are indebted to the Editor F. Berra, C. V. Ullmann and the anonymous reviewer for useful suggestions that greatly improved the manuscript. We are grateful to A. Vescogni, C.A. Papazzoni, A. Cipriani and C. Grillenzoni for useful discussions and suggestions in sample preparation and taxonomic interpretation. We thank J.M. McArthur for providing the look-up table version 5.

References

Amorosi A. (1997) - Miocene shallow-water deposits of the northern Apennines: a stratigraphic marker across a dominantly turbidite foreland-basin successions. *Geol. Mijn.*, 75: 295-307.

Bassant P., Van Buchem F.S.P., Strasser A. & Görür N. (2005) - The stratigraphic architecture and evolution of the Burdigalian carbonate-siliciclastic sedimentary systems of the Mut Basin, Turkey. *Sediment.Geol.*, 173(1): 187-232.

Benisek M.F., Betzler C., Marcano G. & Mutti M. (2009) - Coralline-algal assemblages of a Burdigalian platform slope: implications for carbonate platform reconstruction (northern Sardinia, western Mediterranean Sea). *Facies*, 55(3): 375-386.

Bernoulli D. (2001) - Mesozoic-Tertiary carbonate platforms, slopes and basins of the external Apennines and Sicily. In: Vai G.B. & Martini I.P. (Eds) - Anatomy of an Orogen: the Apennines and Adjacent Mediterranean Basins: 307-326, Kluwer Acadamic Publishers.

Betzler C., Brachert T.C., Braga J.C. & Martìn J.M. (1997) - Nearshore, temperate, carbonate depositional systems (lower Tortonian, Agua Amarga Basin, southern Spain): implications for carbonate sequence stratigraphy. *Sediment. Geol.*, 113: 27-53.

Bicchi E., Dela Pierre F., Ferrero E., Maia F., Negri A., Pirini Radrizzani C., Radrizzani S. & Valleri G. (2006) -Evolution of the Miocene carbonate shelf of Monferrato (North-western Italy). *Boll. Soc. Paleontol. It.,* 45(2):171-194.

Braga J.C., Martin J.M.M., Betzler C. & Aguirre J. (2006) - Models of temperate carbonate deposition in Neogene basins in SE Spain: a synthesis. In: H.M. Pedley & G. Carannante (Eds) - Cool-water carbonates: depositional systems and palaeoenvironmental controls. *Geol. Soc. London Spec. Publ.*, 255: 121-135.

Brandano M. & Policicchio G. (2012) - Strontium stratigraphy of the Burdigalian transgression in the Western Mediterranean. *Lethaia*, 45(3): 315-328.

Brandano M. & Ronca S. (2014) - Depositional processes of the mixed carbonate-siliciclastic rhodolith beds of the Miocene Saint-Florent Basin, northern Corsica. *Facies*, 60(1): 73-90.

Browning J.V., Miller K.G., Sugarman P.J., Barron J., McCarthy F.M., Kulhanek D.K., Katz M.E. & Feigenson M.D. (2013) - Chronology of Eocene–Miocene sequences on the New Jersey shallow shelf: Implications for regional, interregional, and global correlations. *Geosphere*, 9: 1434-1456.

Capo R.C., Stewart B.W. & Chadwick O.A. (1998) - Strontium isotopes as tracers of ecosystem processes: theory and methods. *Geoderma*, 82(1): 197-225.

Carannante G. & Simone L. (1996) - Rhodolith facies in the Central-Southern Apennines Mountains, italy. In: Franseen E.K., Esteban L., Ward W.C. & Rouchy G.M. (Eds) - Models for carbonate Stratigraphy. *SEPM, Concepts Sedimentol. Paleontol.*, 5: 261-275.

Conti S. (1990) - Geologia dell'Appennino marchigiano-romagnolo tra le valli del Savio e del Foglia (Note illustrative alla carta geologica a scala 1:50.000). *Boll. Soc. Geol. It.,* 108: 453-490.

Conti S., Fontana D. & Lucente C.C. (2008) - Sedimentary filling of a wedge-top basin and realationship with the foredeep (Middle Miocene) Marnoso-arenacea Formation, northern Apennines. *Facies*, 54(4): 479-498.

Conti S., Fioroni C., Fontana D. & Grillenzoni C. (2016) - Depositional history of the Epiligurian wedge-top basin in the Val Marecchia area (northern Apennines, Italy): a revision of the Burdigalian-Tortonian succession. *Ital. J. Geosci.*, 135(2): 324-335.

Conti S., Fioroni C. & Fontana D. (2017) - Correlating shelf carbonate evolutive phases with fluid expulsion episodes in the foredeep (Miocene, northern Apennines, Italy). *Mar. Pet. Geol.,* 79: 351-359.

De Capoa P., D'Errico M., Di Staso A., Perrone V., Perrotta S. & Tiberi V. (2015) - The succession of the Val Marecchia Nappe (Northern Apennines, Italy) in the light of new field and biostratigraphic data. *Swiss J. Geosci.*, 108(1): 35-54.

De Paolo D.J. & Ingram B.L. (1985) - High-resolution stratigraphy with strontium isotopes. *Science*, 227(4689): 938-941.

Eidvin T., Ullmann C.V., Dybkjær K., Rasmussen E.S. & Piasecki S. (2014) - Discrepancy between Sr isotope and biostratigraphic datings of the upper middle and upper Miocene successions (Eastern North Sea Basin, Denmark). *Palaeogeogr., Palaeoclimatol., Palaeoecol.*, 411: 267-280.

Fontana D., Conti S., Fioroni C. & Grillenzoni C. (2015) - Factors controlling the evolution of a wedge-top temperate-type carbonate platform in the Miocene of the northern Apennines (Italy). *Sediment. Geol.*, 319: 13-23.

Fornaciari E., Di Stefano A., Rio D. & Negri A. (1996) - Middle Miocene quantitative calcareous nannofossil biostratigraphy in the Mediterranean region. *Micropaleontology*: 42: 137-163.

Freitas P.S., Clarke L.J., Kennedy H., Richardson C.A. & Abrantes F. (2006) - Environmental and biological controls on elemental (Mg/Ca, Sr/Ca, and Mn/Ca) ratios in shells of the king scallop *Pecten maximus*. *Geochim. Cosmochim. Acta*, 70: 5119-5133.

Freitas P.S., Clarke L.J., Kennedy H.A. & Richardson C.A. (2008) - Inter- and intra-specimen variability masks reliable temperature control on shell Mg/Ca ratios in laboratory and field cultured *Mytilus edulis* and *Pecten maximus* (bivalvia). *Biogeosci. Discuss.*, 5: 531-572.

Hodell D.A. & Woodruff F. (1994) - Variations in the strontium isotopic ratio of seawater during the Miocene: Stratigraphic and geochemical implications. *Paleoceanography*, 9(3): 405-426.

Howarth R.J. & McArthur J.M. (1997) - Statistics for strontium isotope stratigraphy: A robust LOWESS fit to the marine Sr-isotope curve for 0 to 206 Ma, with look-up table for derivation of numeric age. *J. Geol.*, 105(4): 441-456.

Krabbenhöft A., Eisenhauer A., Böhm F., Vollstaedt H., Fietzke J., Liebetrau V., Augustin N., Peucker-Ehrenbrink B., Müller M.N., Horn C., Hansen B.T., Nolte N. & Wallmann K. (2010) - Constraining the marine strontium budget with natural strontium isotope fractionations ($^{87}Sr/^{86}Sr^*$, $\delta^{88/86}Sr$) of carbonates, hydrothermal solutions and river waters. *Geochim. Cosmochim. Acta,* 74(14): 4097-4109.

Kroeger K.F., Reuter M., Forst M.H., Breisig S., Hartmann G. & Brachert T.C. (2007) - Eustasy and sea water Sr composition: application to high-resolution Sr-isotope stratigraphy of Miocene shallow-water carbonates. *Sedimentology*, 54(3): 565-585.

Li D., Shields-Zhou G.A., Ling H.F. & Thirlwall M. (2011) - Dissolution methods for strontium isotope stratigraphy: Guidelines for the use of bulk carbonate and phosphorite rocks. *Chemical Geology*, 290(3): 133-144.

Longman M.W. (1980) - Carbonate diagenetic textures from nearsurface diagenetic environments. *AAPG Bulletin*, 64(4): 461-487.

Marroni M. & Pandolfi L. (2007) - The architecture of an incipient oceanic basin: a tentative reconstruction of the Jurassic Liguria-Piemonte basin along the Northern Apennines–Alpine Corsica transect. *Int. J. Earth Sci.*, 9: 1059-1078.

Marshall J.D. (1992) - Climatic and oceanographic isotopic signals from the carbonate rock record and their preservation. *Geological magazine*, 129(2): 143-160.

Martinuš M., Fio K., Pikelj K. & Aščić Š. (2013) - Middle Miocene warm-temperate carbonates of Central Paratethys (Mt. Zrinska Gora, Croatia): paleoenvironmental reconstruction based on bryozoans, coralline red algae, foraminifera, and calcareous nannoplankton. *Facies*, 59(3): 481-504.

McArthur J.M. (1994) - Recent trends in strontium isotope stratigraphy. *Terra Nova*, 6: 331-358.

McArthur J.M., Howarth R.J. & Bailey T.R. (2001) - Strontium isotope stratigraphy: LOWESS version 3: best fit to the marine Sr-isotope curve for 0–509 Ma and accompanying look-up table for deriving numerical age. *J. Geol.*, 109: 155-170.

McArthur J.M., Howarth R.J. & Shields G.A. (2012) - Strontium isotope stratigraphy. In: Gradstein F.M., Ogg J.G., Schmitz M.D. & Ogg G.M. (Eds) - The geologic timescale 2012: 127-144, Elsevier.

Molli G. (2008) - Northern Apennine-Corsica orogenic system: an updated overview. In: Siegesmund S., Fugenshuh B. & Froitzheim N. (Eds) - Tectonic Aspects of the Alpine-Dinaride-Carpathian System. *Geol. Soc. London Spec. Publ.*, 298: 413-442.

Mutti M., Piller W.E. & Betzler C. (2010) - Miocene carbonate systems: an introduction. In: Mutti M., Piller W.E. & Betzler C. (Eds) - Oligocene-Miocene Carbonate Systems, *IAS Spec. Publ.*, 42: vii–xii.

Palmiotto C., Corda L., Ligi M., Cipriani A., Dick H.J.B., Douville E., Gasperini L., Montagna P., Thil F., Borsetti A.M., Balestra B. & Bonatti E. (2013) - Nonvolcanic tectonic islands in ancient and modern oceans. *Geochem., Geophys., Geosyst.*, 14(10): 4698-4717.

Pomar L., Bassant P., Brandano M., Ruchonnet C. & Janson X. (2012) - Impact of carbonate producing biota on platform architecture: insights from Miocene examples of the Mediterranean region. *Earth-Sci. Rev.*, 113(3): 186-211.

Reuter M., Piller W.E., Brandano M. & Harzhauser M. (2013) - Correlating Mediterranean shallow water deposits with global Oligocene-Miocene stratigraphy and oceanic events. *Glob. Planet. change*, 111: 226-236.

Ricci Lucchi F. (1964) - Ricerche sedimentologiche sui lembi alloctoni della Val Marecchia (Miocene inferiore e medio). *Giornale di Geologia*, 32: 546-652.

Ricci Lucchi F. (1986) - The Oligocene to Recent foreland basins of the northern Apennines. In: Allen P.A. & Homewood P. (Eds) - Foreland Basins, *IAS Spec. Publ.*, 8: 105-139.

Ricci Lucchi F. (1990) - Turbidites in foreland and on-thrust basins of the Northern Apennines. *Palaeogeogr., Palaeoclimatol., Palaeoecol.*, 77: 51-66.

Ruggieri G. (1954) - Il lembo parautoctono di Montebello (Val Marecchia). *Boll. Serv. Geol. It.*, 75: 615-632.

Salocchi A.C., Argentino C. & Fontana D. (2017) - Evolution of a Miocene carbonate shelf (northern Apennines, Italy) revealed through a quantitative compositional study. *Mar. Pet. Geol.*, 79: 340-350.

Scasso R.A., McArthur J.M., Del Rıo C.J., Martınez S. & Thirlwall M.F. (2001) - $^{87}Sr/^{86}Sr$ Late Miocene age of fossil molluscs in the 'Entrerriense' of the Valdés Peninsula (Chubut, Argentina). *J. S. Am. Earth Sci.*, 14(3): 319-329.

Schneider S., Fürsich F.T. & Werner W. (2009) - Sr-isotope stratigraphy of the Upper Jurassic of central Portugal (Lusitanian Basin) based on oyster shells. *Int. J. Earth Sci.*, 98(8): 1949-1970.

Steiger R.H. & Jäger E. (1977) - Subcommission on geochronology: convention on the use of decay constants in geo- and cosmochronology. *Earth Planet. Sc. Lett.,* 36: 359-362.

Ullmann C.V. & Korte C. (2015) - Diagenetic alteration in low-Mg calcite from macrofossils: a review. *Geol. Quart.*, 59(1): 3-20.

Ullmann C.V., Böhm F., Rickaby R.E., Wiechert U. & Korte C. (2013) - The Giant Pacific Oyster (*Crassostrea gigas*) as a modern analog for fossil ostreids: Isotopic (Ca, O, C) and elemental (Mg/Ca, Sr/Ca, Mn/Ca) proxies. *Geochem., Geophy., Geosyst.*, 14(10): 4109-4120.

Veizer J. (1983) - Trace elements and isotopes in sedimentary carbonates. *Rev. Mineral. Geochem.*, 11(1): 265-299.

Veizer J., Buhl D., Diener A., Ebneth S., Podlaha O.G., Bruckschen P., Jasper T., Korte C., Schaaf M., Ala D. & Azmy K. (1997) - Strontium isotope stratigraphy: potential resolution and event correlation. *Palaeogeogr., Palaeoclimatol., Palaeoecol.,* 132(1): 65-77.

Vescogni A., Bosellini F.R., Cipriani A., Gürler G., Ilgar A. & Paganelli E. (2014) - The Dağpazarı carbonate platform (Mut Basin, Southern Turkey): Facies and environmental reconstruction of a coral reef system during the Middle Miocene Climatic Optimum. *Palaeogeogr., Palaeoclimatol., Palaeoecol.*, 410: 213-232.